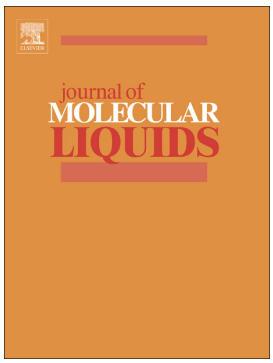

Biogenic palladium nanoclusters supported on hybrid nanocomposite 2-hydroxypropyl-β-cyclodextrin/alginate as a recyclable catalyst in aqueous medium

Thanh-Danh Nguyen, Thanh-Truc Vo, Cao-Hien Nguyen, Van-Dat Doan, Chi-Hien Dang

PII: S0167-7322(18)34539-2
DOI: https://doi.org/10.1016/j.molliq.2018.12.138
Reference: MOLLIQ 10214

To appear in: *Journal of Molecular Liquids*

Received date: 3 September 2018
Revised date: 5 November 2018
Accepted date: 26 December 2018

Please cite this article as: Thanh-Danh Nguyen, Thanh-Truc Vo, Cao-Hien Nguyen, Van-Dat Doan, Chi-Hien Dang , Biogenic palladium nanoclusters supported on hybrid nanocomposite 2-hydroxypropyl-β-cyclodextrin/alginate as a recyclable catalyst in aqueous medium. Molliq (2018), https://doi.org/10.1016/j.molliq.2018.12.138

Biogenic palladium nanoclusters supported on hybrid nanocomposite 2-hydroxypropyl-*β*-cyclodextrin/alginate as a recyclable catalyst in aqueous medium

Thanh-Danh Nguyen [a,b]*, Thanh-Truc Vo[b,c], Cao-Hien Nguyen[c,d], Van-Dat Doan[e] and Chi-Hien Dang[b,c]

[a]Institute of Research and Development, Duy Tan University, Da Nang City, Vietnam.

[b]Institute of Chemical Technology, Vietnam Academy of Science and Technology, 1 Mac Dinh Chi Street, District 1, Ho Chi Minh City, Vietnam.

[c]Graduate University of Science and Technology, Vietnam Academy of Science and Technology, 18 Hoang Quoc Viet, Cau Giay, Hanoi, Vietnam.

[d]Department of Chemical Technology, Ho Chi Minh City University of Food Industry, Ho Chi Minh, Vietnam.

[e]Faculty of Chemical Engineering, Industrial University of Ho Chi Minh city, Ho Chi Minh city, Vietnam.

***Corresponding author:** Thanh-Danh Nguyen, Fax: (+84)-8.38238265; Email: danh5463bd@yahoo.com

Graphic Abstract

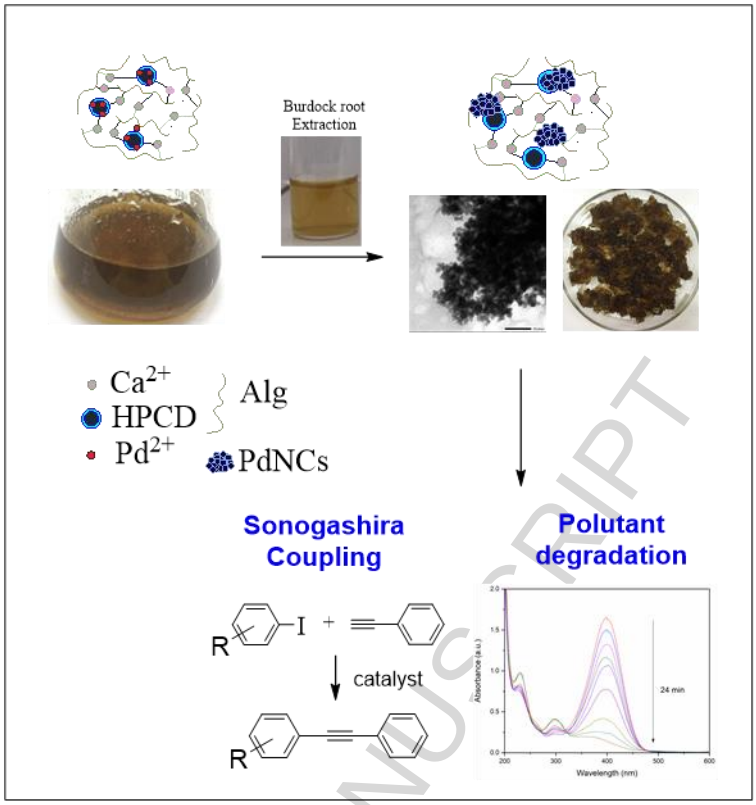

Graphical abstract

Keywords: palladium nanoclusters, nanocomposite, biosynthesis, catalysis, *Arctium lappa*.

Abstract

This paper develops a simple and green process of synthesizing palladium nanoclusters (PdNCs) capped on the hybrid nanocomposite based on biodegradable polysaccharides, 2-hydroxypropyl-β-cyclodextrin (HPCD) and alginate (Alg) through an ionotropic gelation mechanism. PdNCs were biosynthesized from aqueous extract of Burdock root (BR), *Arctium lappa*. The nanocomposite PdNCs/HPCD/Alg was characterized by techniques like UV-vis, FTIR, EDX, FESEM, TEM, HR-TEM and TG-DTA. The crystal palladium nanoparticles were found to distribute in cluster shape with a size of 4-10 nm. EDX data showed that average amount of palladium capped on the hybrid nanocomposite was approx. 4.7 % (w/w). PdNCs/HPCD/Alg exhibited highly catalytic activity for degradation of

pollutants including 4-nitrophenol, methyl orange and rhodamine B in wastewater and leaching mechanism of the nanocatalyst was showed. In particular, the nanocomposite showed excellent aqueous-phase catalytic performance for free-triphenylphosphine Sonogashira cross-coupling reaction. The nanocatalyst could be efficiently reused without much compromising with its activity.

1. Introduction

Metallic nanoparticles (MNPs) have significant attentions due to their various applications including biomaterials, catalyst and electrochemical applications [1,2]. In particular, palladium nanoparticles (PdNPs) are very popularly used as catalyst for organic reactions due to high performance compared to the traditional catalysts [3,4]. PdNPs with diameters less than 10 nm possessing high surface to volume ratio, thus providing many highly active metal uncoordinated sites, were widely used within cross-coupling reactions and especially, degradation of environmental pollutants [5,6]. PdNCs received considerable attentions as efficient catalysts in organic synthesis [7,8]. However, environmental effects, production cost and reused issues still are major barriers for their widespread application in the industry.

The recent researches showed that MNPs capped on the biodegradable polysaccharides including starch [9-11], cellulose [12,13], cyclodextrins (CDs) [14-16] and alginate (Alg) [17-20] have displayed high catalytic activities and possess many advantages. Among of them, the cyclodextrins (CDs) and alginate (Alg) are specifically interested due to their capping and stabilization. For example, CDs can load small molecules and nanometallic materials to form inclusion complexes [21]. Meanwhile, Alg is well-known as biocarriers of MNPs to fabricate biofilms [22].

PdNPs capped on CD-based carriers exhibited various applications including catalyst, and electrochemical materials [23,24]. The recent researches showed PdNPs could be

synthesized *in situ* using HPCD or β-CD as the reducing and stabilizing agents and their applications in the cross-coupling reactions [25,26]. CDs attaching perthiol groups are recently used an effective method to support PdNPs [27-29], however, it has exhibited to be a complex multi-step way. On the other hand, PdNPs loaded onto alginate-based composite could be synthesized by using green techniques such as microwave [30] and bacteria [31]. Recently, PdNPs/Alg are considered for removal of the toxic pollutants in treatment of wastewater [32,33]. However, recyclability of palladium/polysaccharides nanocatalyst in water medium is very low due to high solubility of these polysaccharides.

Our recent study showed that the nanocomposite HPCD/Alg could be simply synthesized via the ionotropic gelation mechanism and efficiently capping biogenic MNPs [34, 35]. This nanocomposite can be considered as a novel method for trapping the metallic ions and converting into MNPs. The nanocomposite AgNPs/HPCD/Alg exhibited many advantages of catalyst in water medium including good colloid disperse and high recyclability. On the other hand, aqueous extract of Burdock root (BR), *A. lappa* has shown as an effective reductant for biosynthesis of MNPs [36]. In aim of this work to enhance activity and recyclability of green-synthesized nanometal catalysts, we report biogenic PdNCs capped into the nanocomposite prepared from HPCD and alginate which are synthesized from aqueous extract of Burdock root (BR), *A. lappa*. This method should be considered as a green approach for synthesis of nanometal due to low-cost procedure and friendly-environmental used materials. Recyclable catalytic performance of the nanocomposite for degradation of pollutants and Sonogashira cross-coupling as model reactions has been evaluated.

2. Materials and methods

2.1. Materials

All chemicals were used as received without further purification. The major reagents including 2-hydroxypropyl-β-cyclodextrin (HPCD), sodium alginate, palladium acetate ($Pd(OAc)_2$), 4-nitrophenol (4-NP), methyl orange (MO), rhodamine B (RhB), sodium borohydride ($NaBH_4$) and calcium chloride ($CaCl_2$) were purchased from Acros (Belgium). Burdock root (BR), *A. lappa* was purchased from Khai Minh Macrobiotics (Ho Chi Minh city). Deionized water was used throughout.

2.2. Synthesis of PdNCs/HPCD/Alg

Aqueous extract of BR and blank HPCD/Alg were prepared as previous report [35,36]. Synthesis of the nanocomposites was performed via the ionotropic gelation method. In the present work, a feeding rate of Pd^{2+} ions (5%, w/w) was deposited in the nanocomposite. 50.0 mL of aqueous calcium chloride (14.0 mg mL^{-1}) was dropped into 18.6 mL of sodium alginate solution (28.0 mg mL^{-1}) under stirring for 60 min at 1200 rpm. The Alg/Ca^{2+} gelispheres were centrifugated by EBA20S-Hettich Germany at 8,000 rpm, at 30 ^oC for 30 min and washed with the deionized water (3x20 mL) to remove the impurities. Meanwhile, solution of $Pd(OAc)_2$ in DMSO (5.0 mL, 31.3 mg mL^{-1}) was dropped to HPCD solution (100 mL, 3.50 mg mL^{-1}) and stirred for 60 minutes at 1200 rpm. Then, the Pd^{2+}/HPCD solution was dispersed into the Ca^{2+}/Alg gelispheres. The nanocomposite mixture was stirred in an hour and equilibrated overnight. The nanocomposite was centrifugated at 8,000 rpm for 30 min and washed with DMSO (3x20 mL) and water (3x20 mL). The resulting gel was dissolved again into the deionized water (100 mL) under stirring.

2.0 mL of the BR extract was dropped into the gel solution in dark at 90^oC. The PdNCs formed could be visually observed by changes in the UV-vis spectra. The PdNCs/HPCD/Alg nanocomposite was obtained by centrifugation technique (10,000 rpm, 30 min) and washed with DMSO (3 x 10 mL) and deionized water (3 x 10 mL) for removal of the impurities.

Then, dry powder of PdNCs/HPCD/Alg catalyst was obtained from drying at 90^{o}C in the air atmosphere for overnight.

2.3. Physicochemical characterization of PdNCs/HPCD/Alg

UV-Vis Spectra were measured on JASCO V-630 spectrophotometer (U.S.A) at the range between 200 and 600 nm wavelengths. The Fourier-transform infrared (FTIR) spectra of the plant extract, blank HPCD/Alg and PdNCs/HPCD/Alg samples were determined by a Bruker, Tensor 27 FTIR spectrophotometer (Germany) with the wavelength ranging from 500 to 4000 cm^{-1}. The morphology and size distribution of the biosynthesized nanocomposite were measured by using FESEM (JSM7401F, Japan) and TEM (Hitachi H8100). The crystal structure analysis of atoms was determined on HRTEM, (JEOL JEM2100). Energy dispersive X-ray spectroscopy (EDX) analyzer (Horiba, EMAX ENERGY EX-400) was used to analyze chemical elements in micro-area and elemental distribution in the nanocomposite. For measurements of particle size and zeta potential, the nanocomposite solutions were measured by using analyzer, nanoPartica Horiba SZ-100 (Japan) at 25^{o}C. A LabSys evo S60/58988 Thermoanalyzer (Setaram, France) was used for simultaneous thermal analysis combining thermogravimetry (TG) analysis and different thermal analysis (DTA) in temperature range from room temperature to 800^{o}C at a heating rate of 10^{o}C/min in the air atmosphere.

2.4. Catalytic activity for degradation of pollutants

The catalytic activity of PdNCs/HPCD/Alg was evaluated by degradation of organic pollutants including (4-NP), methyl orange (MO) and rhodamine B (RhB) in water with excess amount of $NaBH_4$. The mixture containing the pollutants (2.5 mL, 0.1 mM) and $NaBH_4$ (0.5 mL, 0.06 M) was added into a quartz cell (1 cm path length). Then, the biosynthesized nanocomposite powder (1 mg) were added into the reaction mixture. The degradation of the pollutants with different reaction time was monitored by UV-Vis

spectrophotometer in the range between 200 and 800 nm wavelengths at the room temperature. After addition of the nanocomposite was completed, a rapid decrease in intensity of the absorption peaks at 400, 464 and 554 nm was observed for degradation of 4-NP, MO and RhB, respectively.

For study of degradation kinetics, the reaction rate should depend on the concentrations of reactants as well as catalysts. However, to reduce influence of the factors, the present work used high concentration of $NaBH_4$ and very low concentration of the nanocomposite catalyst in comparison with the pollutants. The reaction rate, thus, is independent from the concentrations of $NaBH_4$ and the catalyst. As a result, their degradation should be considered as a pseudo first-order reaction with respect to the concentration of the pollutants [37]. The reaction kinetic can be described by the equation $\ln (A_t/A_0) = - kt$, where k is pseudo-first order rate constant, t is the reaction time, $[A_0]$ is the concentration of the pollutants at time t = 0 and $[A_t]$ is the concentration at time 't'. The pseudo-first order rate constant k can be found directly from the slope of straight line yielded by plots of $\ln(A_t/A_0)$ versus reaction time.

For evaluation of catalytic recyclability, after each cycle, the nanocomposite samples were collected from the quartz cell and washed several times with deionized water before reuse.

2.5. Catalytic activity for Sonogashira Coupling

To a freshly prepared solution of the nanocomposite powder (5.0 mg) in water (3 mL), base (4 mmol) and CuI (0.10 mmol) was added and followed by iodobenzene derivatives (0.10 mmol) and phenylacetylene (0.1 mmol). Then, the reaction mixture was stirred in the air atmosphere. After completion of the reaction, monitored by TLC, the product was extracted with ethyl acetate. The organic layer was washed with water, dried over $MgSO_4$ and concentrated *in vacuo*. The crude product purified by flash column

chromatography on silica gel (0.06-0.2 mm) with *n*-hexane/ethyl acetate from 100:1 to 95:5 (v/v) as the eluents. The purity of product was determined by ^{1}H and ^{13}C-NMR measurements. For catalytic recycle, the catalyst was collected from water layer after extract of hexane by centrifugation technique and then washed several times with deionized water before reuse.

3. Results and Discussion

3.1.Biosynthesis of the nanocomposites

The route of this work is illustrated in Figure 1. The nanocomposites based on HPCD/Alg were prepared via the inotropic gelation mechanism which proposed that some cross-link of alginate and calcium ions in the galispheres Alg/Ca^{2+} was replaced by HPCD molecules in aqueous medium [34]. The Pd^{2+} ions were loaded onto the nanocomposite HPCD/Alg via the chemical bonds to form the composite Pd^{2+}/HPCD/Alg. Because attempts on *in situ* reduction of Pd^{2+}/HPCD/Alg gel solution without any reductant has been failed, the aqueous extraction of BR containing polyphenols was used as an environmentally friendly reductant for synthesis of the biogenic nanocomposite, PdNCs/HPCD/Alg [35]. The formation of PdNCs might be visibly recognized by change from UV-vis spectra in the 200 – 600 nm range (Figure 1). The UV-vis spectrum of blank HPCD/Alg displayed almost no absorbance bands. The absorption bands at range 320-400 nm were ascribed to charge-transfer transition of ion Pd^{2+} capped on HPCD/Alg. For the reduced samples, the disappearance of these absorption bands suggested a complete reduction of the Pd^{2+} ions by the aqueous extraction of BR. In next step, PdNCs/HPCD/Alg was collected and purified by using centrifugation. Finally, the pure nanocomposite powder was used to evaluate the catalytic activity in degradation of pollutants and Sonogashira cross-coupling reactions in water.

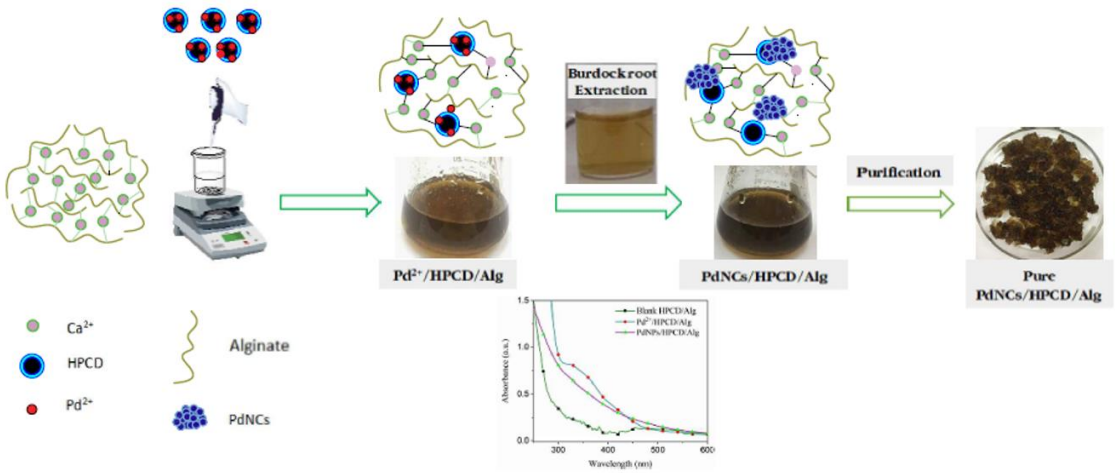

Figure 1. Schematic illustration of preparation of PdNCs/HPCD/Alg.

3.2.Physicochemical characterizations of catalyst

The IR spectra were measured to identify the functional groups present in the BR extract and the biosynthesized composites as shown in Figure 2. The blank and biosynthesized composites showed similar absorption bands. The absorption band characteristics of the blank nanocomposite were observed at 3422 cm^{-1} corresponded to OH group and the peaks near 1615 cm^{-1} and 1418 cm^{-1} assigned to symmetric and asymmetric stretching vibration of COO^- groups, respectively [38]. The peaks of the blank nanocomposites have been known to relate to the corresponding functional groups of alginate structure [34]. In aqueous extract of BR, the bands were observed at 1033, 1336, 1430, 1633, 2870, 2932 and 3375 cm^{-1}. These bands are attributed to the presence of polyphenol and proteins that play a role as the reductants in synthesis of the nanocomposite PdNCs/HPCD/Alg [39, 40]. After completed reduction, spectrum of the biosynthesized nanocomposite was slightly shifted to new positions compared to peaks of the blank nanocomposite e.g. bands at 1621 and 1424 cm^{-1}.

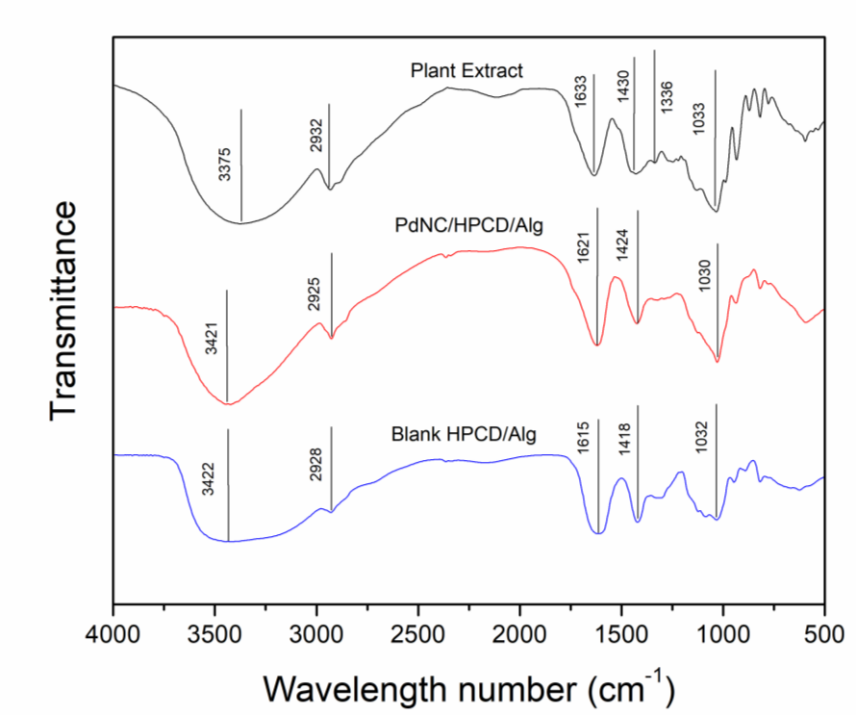

Figure 2. FT-IR spectra of blank HPCD/Alg, PdNCs/HPCD/Alg and BR extract.

Figure 3 showed the elemental composition of the nanocomposite PdNCs/HPCD/Alg using EDX spectrum which was plotted in ionization energy versus intensity of X-rays. The average elemental composition was calculated in percental type of weight per weight (inset of Figure 3). The EDX spectrum proved the presence of relating elements in the nanocomposite. The signals corresponding to elemental carbon and oxygen revealed possibly organic components in the nanocomposite. Additionally, presence of calcium element indicated presence of cross-link between Ca^{2+} ions and alginate in the nanocomposite. Calculation from EDX data showed average value of approx. 4.7 % (w/w) of palladium in the nanocomposite.

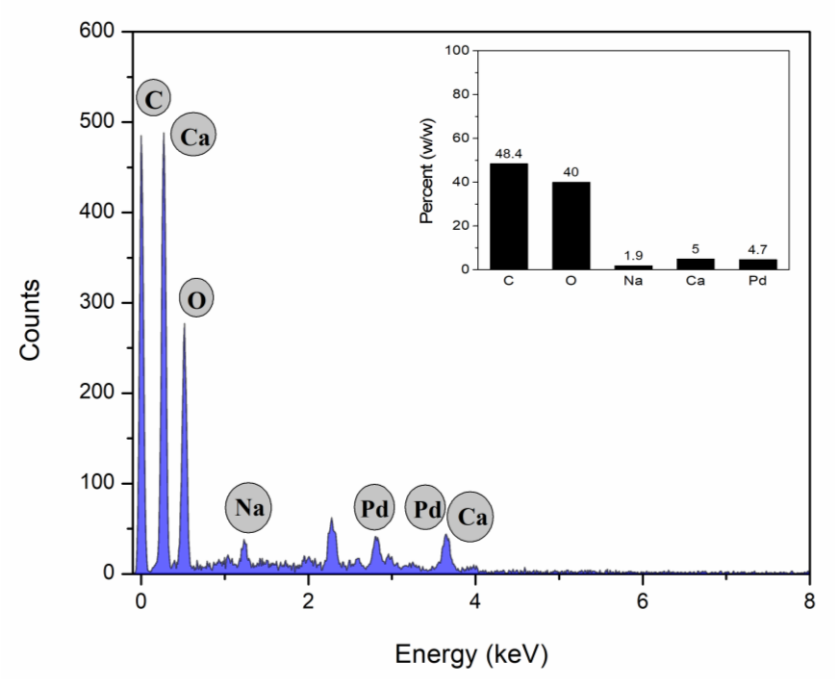

Figure 3. EDX spectrum and average content of elements (inset) of nanocomposite PdNCs/HPCD/Alg.

For studies on morphology of the nanocomposite, its film and powder are observed by FESEM technique. The film was fabricated from aqueous solution in vacuum at the room temperature while powder of the nanocomposite was dried in oven at 100^{o}C in the air atmosphere. Measurement of the film (Figure 4A) shows smooth surfaces with tiny holes which can be formed from rapid evaporation of water molecules in the vacuum. It indicated that the films with a good surface can be fabricated easily from the nanocomposite in vacuum. In contrast, FESEM image of the nanocomposite powder exhibits the rough surfaces with obvious mounds, indicated successful formation of cross-links between calcium ions with alginate and HPCD molecules. TEM image showed that the nanocomposite capped successfully palladium with the cluster shape of agglomerated palladium particles in diameter range of 4-10 nm. Crystal structure of the PdNCs is clearly observed in SAED pattern and HRTEM image (Figure 4E) that displays the fringe lattice of the palladium nanoparticles with a spacing of 0.2 nm. The STEM and EDX mapping images (Figures 4F & G) of the nanocomposite reveal presence of Pd, C, O and Ca elements,

indicated that the PdNPs bind to the carrier based on alginate and HPCD molecules with cross-links formed by calcium ions.

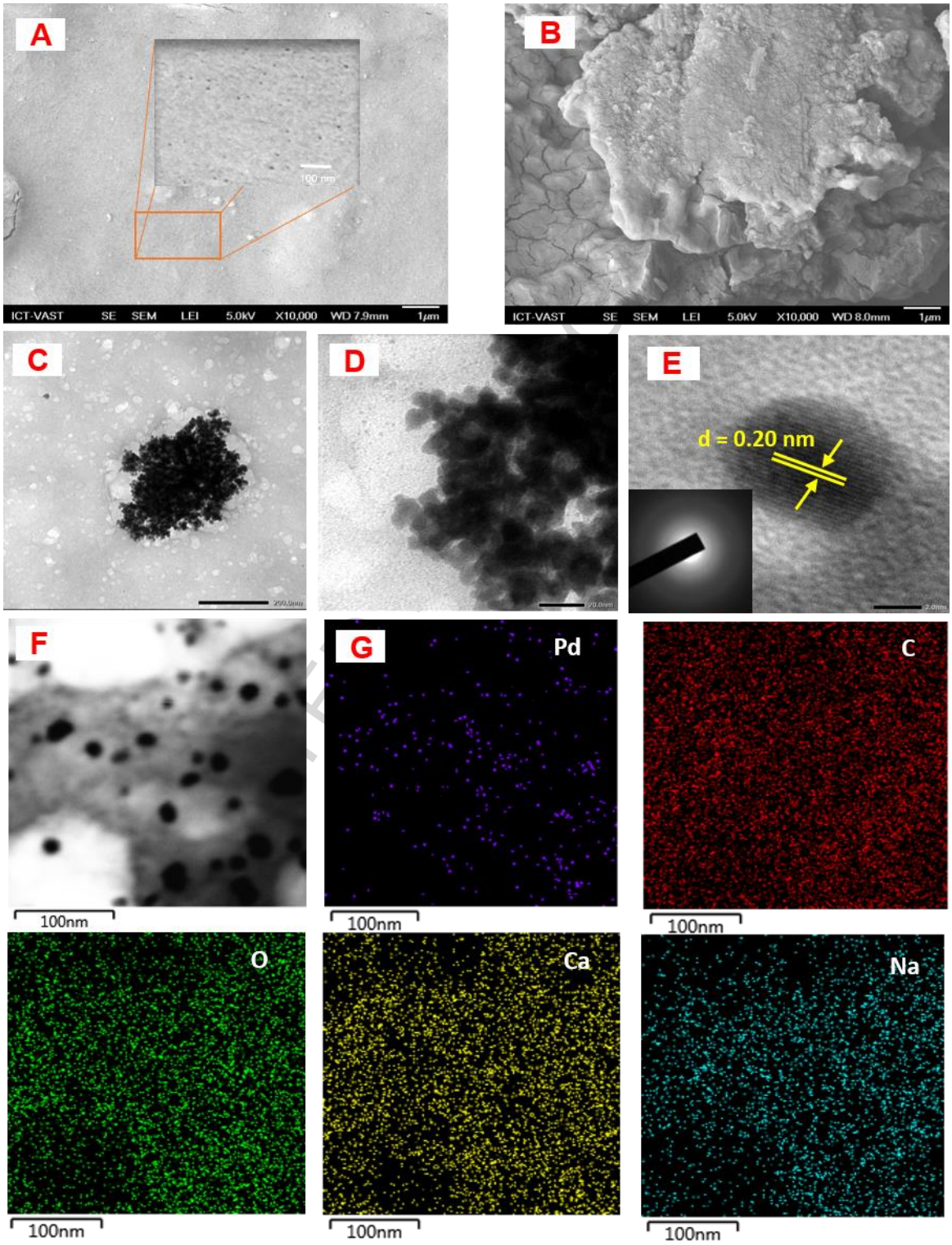

Figure 4. FESEM images of PdNCs/Alg/HPCD fabricated at room temperature under vacuum (A) and at 100°C in the air atmosphere (B), TEM images in different magnifications (C and D), HRTEM image (E) and SAED pattern (inset), STEM image (F) and EDX mapping images (G).

To study stability and size distribution of the nanocomposite in the aqueous medium, measurement of dynamic light scattering (DLS) and zeta potential was carried out at 25°C as shown in Figure 5 [41]. Our previous research[35] showed that the blank HPCD/Alg possessed zeta potential value of -40.0 mV and polydispersed distribution with mean hydrodynamic diameters of 28.3 nm and 1250.3 nm. In the present study, the negative charge at the electrical double layer surrounding the biosynthesized nanocomposite PdNCs/HPCD/Alg (-75.9 mV) is significantly higher than that of the blank nanocomposite solution (Figure 5A). The result confirmed the nanocomposite possessing the high stability in water. The size distribution profile (Figure 5B) showed that the nanocomposite PdNCs/HPCD/Alg was monodispersed with a mean hydrodynamic diameter of 89.2 nm which was much greater than diameter of the AgNPs/HPCD/Alg (9.8 nm) in the previous report [35].

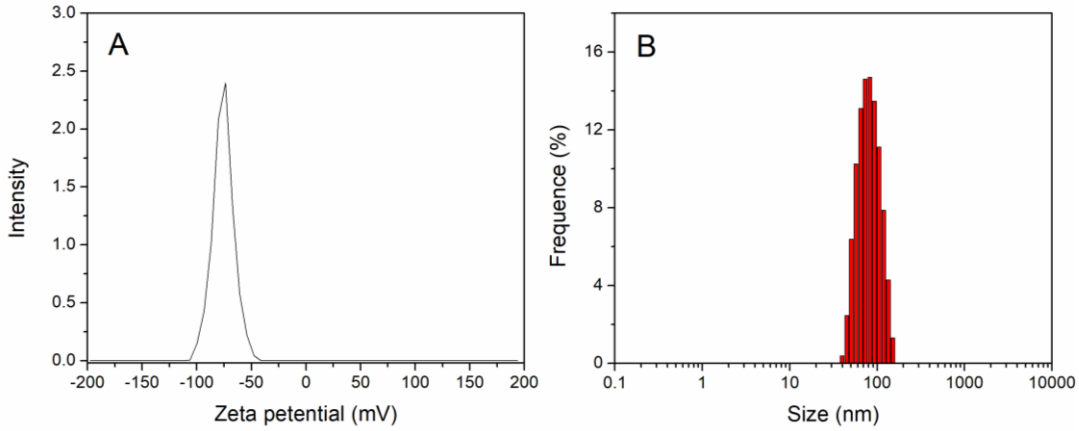

Figure 5. Zeta potential (A) and dynamic light scattering (B) of PdNCs/HPCD/Alg

For thermal behaviors of the nanocomposite, TG–DTA curves are simultaneously measured at the heating rate of 10 ∘C/min in the air atmosphere (Figure 6). TG curves of the

nanocomposites, blank HPCD/Alg and PdNCs/HPCD/Alg show thermal decomposition occurred in three stages. Both nanocomposites reveal an initial weight loss of 12 % from 50 to 200°C, assigned to the loss of adsorbed water and volatile components [42]. After this period, thermal decomposition of PdNCs/HPCD/Alg sample occurs in second stages between 210 and 400°C (43%) while this stage of the blank sample is between 230 and 560°C (38 %). In the final stage, mass loss of both nanocomposites was similar and accounted for 30 % of the total weight whereas the thermal stability of the nanocomposite PdNCs/HPCD/Alg (430 °C) is lower significantly than that of alginate (550 °C). Also, DTA curve of the nanocomposite PdNCs/HPCD/Alg shows two maximum exothermic peaks (T_{exo}) at 459 and 546 °C which are significantly lower than T_{exo} value of the blank HPCD/Alg sample (572 °C). It can be because the presence of palladium induces subversion of cross-links formed from alginate and calcium ions, led to reduction of thermal stability of the nanocomposite PdNCs/HPCD/Alg.

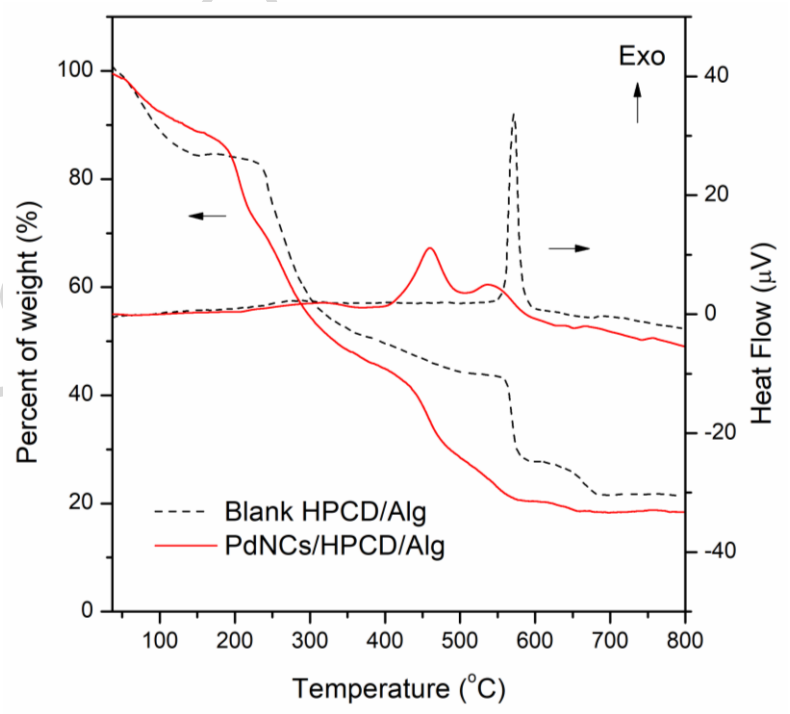

Figure 6. Simultaneous TG-DTA curves of blank HPCD/Alg and PdNCs/HPCD/Alg in air flow of 20 mL/min at heating rate of 10◦C/min.

3.3.Catalytic performance for degradation of pollutants

Removal of dye pollutants is particularly important for wastewater treatment in manufacturing industry. The synthetic organic colorants are the largest group of industrial compounds in both number and amount. Degradation of the dye pollutants was well known as thermodynamically spontaneous reactions in the presence of strong reductants like $NaBH_4$ to form small organic molecules and nontoxic species. Unfortunately, the degradation without the catalyst showed very slow reaction rates [35, 43, 44]. Thus, some noble metals with high reactive activity and specific surface area are usually used as catalysts to accelerate the reaction rate.

In the present study, three contaminants with various structures including 4-nitrophenol (4-NP), methyl orange (MO) and rhodamine B (RhB) represented as the most popular classes of pollutants in wastewater are selected to evaluate catalytic degradation performance of PdNCs/HPCD/Alg.

4-NP has been known as a priority pollutant due to high stability in the environment and biodegradable resistance. As soon as the catalyst PdNCs/HPCD/Alg was added to the 4-nitrophenolate solution with the absorption maximum peak at 400 nm, intense yellow color of the solution was gradually reduced. The reduction performance can be evaluated by tracking the changes in the absorbance at 400 nm from the UV-vis spectra (Figure 7). The progressive decrease of absorbance at 400 nm and simultaneous increase of new peak at 298 nm indicated the reduction of 4-NP to form 4-aminophenol (4-AP). The degradation of 4-NP in presence of the nanocomposite was completed in 24 min with almost zero absorbance at 400 nm.

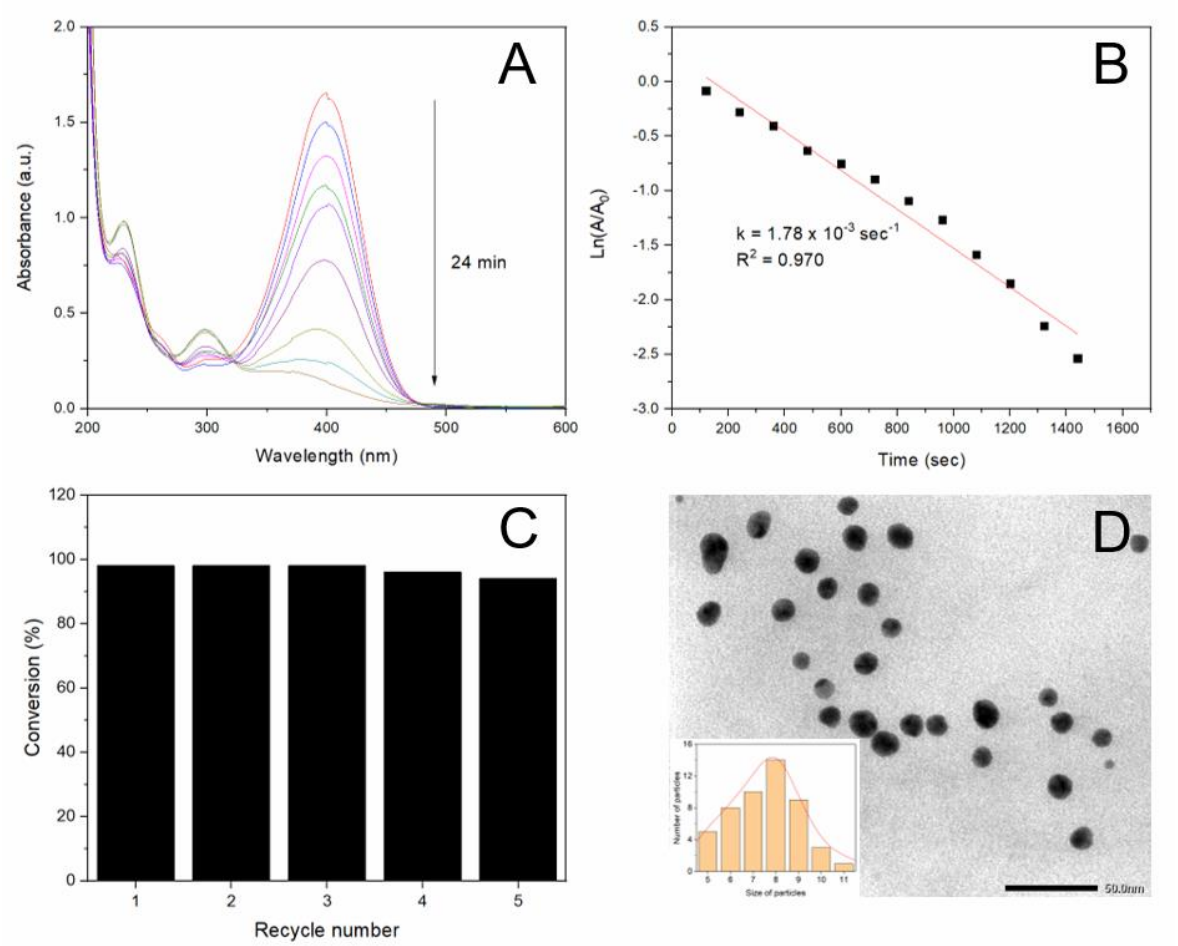

Figure 7. (A) UV-Vis spectra of 4-nitrophenol reduction (B) pseudo first-order kinetic plotted, (C) Conversion efficiency of 4-nitrophenol for five successive reaction cycles in 24 min and (D) TEM image of the catalyst after 5 reaction cycles.

Figure 7B showed the linear relationship for the reduction of 4-NP from plots of $\ln(A_t/A_0)$ versus reaction time, indicated the pseudo first-order reaction. The k value which was determined directly from the slope of plots was 1.78×10^{-3} sec^{-1}. Some rate constants per 1 mg of catalyst in recent studies are listed in Table 1. Taking high k value into account, the catalytic performance of the nanocomposite increased 2-fold in comparison with the catalyst AgNPs/HPCD/Alg [35] and was much superior than other catalysts based on PdNPs [45-47].

Table 1. Comparison of catalytic activity of MNPs@carriers synthesized using different methods towards the reduction of 4-nitrophenol.

MNPs@carrier catalysts	Synthetic method	Rate constant per 1 mg of catalyst (sec^{-1})	References
AgNPs@HPCD/Alg	Biogenic reduction	5.03×10^{-4}	[35]
PdNPs@B.tea	Biogenic reduction	2.95×10^{-4}	[45]
PdNPs@Chitosan	Chemical reduction	1.33×10^{-3}	[46]
PdNPs@MWCNT–APPI	Chemical reduction	9.37×10^{-5}	[47]
PdNCs@HPCD/Alg	Biogenic reduction	1.78×10^{-3}	This work

On the other hand, the recyclability of noble metallic catalyst was very important for the green catalytic application in industry. The prepared nanocomposite PdNCs/HPCD/Alg could be easily separated and purified from the reaction mixture. After each reaction, the nanocatalyst was washed with deionized water and directly used for the next catalysis. In order to test the recyclability of the catalyst, five cyclic reactions were evaluated. As observed in Figure 7C, there is no change in the catalytic efficiency of the nanocomposite after five reaction cycles.

Catalytic activity of PdNCs in cross-coupling reactions can be described by leaching mechanisms which could be demonstrated by changes in particle size before and after the catalyst process [48]. The mechanisms purposed that Pd atoms are leaching out of PdNCs to carry out catalyst before re-cluster process of the leached Pd atoms occurs. The re-cluster process could form new clusters either bigger particle size [49, 50] or smaller particle size [51], depended on the stabilization agents. Meanwhile, the mechanism for degradation of dyes in MNPs catalyst has been well known as an electron transfer process that transferred electrons from the donor BH_4^- ions to the acceptor organic molecules via MNPs surface [52, 53]. However, the mechanism on this degradation reaction in presence of PdNCs catalyst

has not been studied so far. To test changes of the catalyst surface after recycle process, reused catalyst was collected and dissolved again in the distilled water for measurement of TEM image. It showed that morphology of the used catalyst contained separated nanoparticles with an average size of 8.0 nm (Figure 7D). Important differences in morphology of Pd nanocatalyst before (Figure 4) and after catalyst process and almost no change in particle size strongly indicated novel catalytic mechanism of PdNCs in degradation of 4-NP. It is purposed that Pd (0) atoms are leaching out the PdNCs to carry out an electron transfer process in aqueous medium and then, the leached PdNPs cannot recombine to the new nanoclusters (Figure 8). It can be because the reaction products e.g. 4-AP formed new stabilization agents of the PdNPs to prevent this recombination.

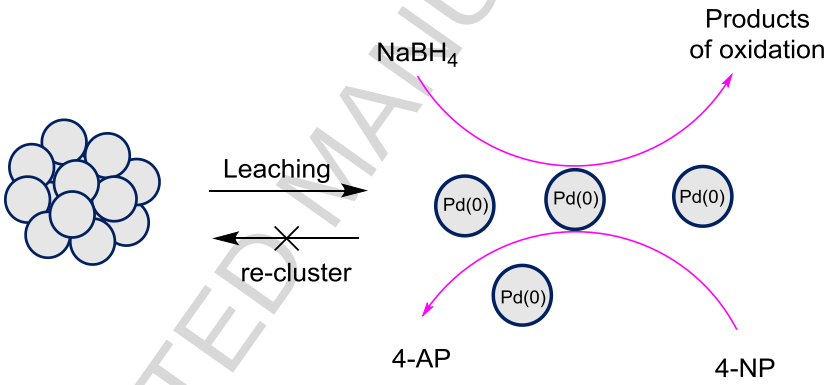

Figure 8. Proposed mechanism for degradation of 4-nitrophenol by the nanocomposite PdNCs/HPCD/Alg

As a representative case of organic azo dye, methyl orange (MO), a common indicator in various analytical fields, was used to evaluate the catalytic activity of PdNCs/ HPCD/Alg. MO is known as a stable pollutant generated several environmental and health problems. The UV-vis absorption band of MO are known to appear at 464 nm. The increased degradation of MO was clearly observed by the color gradually faded after the addition of both $NaBH_4$ and the nanocomposite. Figure 9A showed that the band at 464 nm disappearing within 20 min and simultaneous increase of absorbance at 250 nm indicated efficient

degradation of MO to form new compounds bearing NH_2 groups in presence of the nanocomposite [54]. The k value found from the slope of the linear plot was 2.24 $x10^{-3}$ sec^{-1} with correlation coefficient (R^2) value of 0.992. As revealed in Figure 9C, with the increase of the number of cycles, the conversion efficiency was almost unchanged, demonstrating that PdNCs/HPCD/Alg was not lost its initial catalytic activity and showed good stability after five reaction cycles.

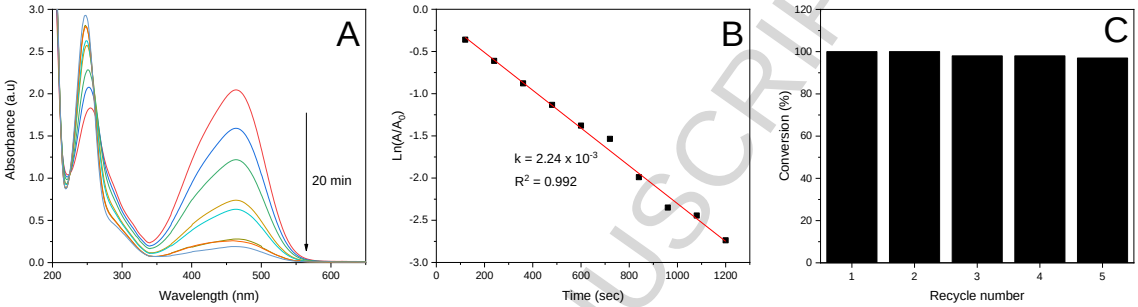

Figure 9. (A) UV-Vis spectra of methyl orange degradation (B) First order kinetic plotted and (C) Conversion efficiency of methyl orange for 5 successive reaction cycles in 20 min.

To demonstrate the nanocomposite has a universal catalytic activity in the decolorization reaction of organic dyes, various kinds of dyes should be studied under the same conditions. Herein, we choose rhodamine B (RhB) as representative model of stable organic dyes with a complex structure for catalytic degradation. RhB is well known as an important dye pollutant and widely employed in textile industries for various purposes. UV-vis absorption characteristics of RhB dye is in maximum bands at 554 nm. The catalytic degradation of RhB in the presence of the nanocatalyst can be observed by the change in color and decreasing absorbance at 554 nm in UV-vis spectra. The results showed that the catalytic degradation of RhB was completed within only 16 min (Figure 10A). The k constant of degradation reaction was found to be 2.75 x 10^{-3} sec^{-1} that demonstrated higher catalytic activity than the nanocomposite, AgNPs/HPCD/Alg [35]. For evaluation of its potential

recyclability, the nanocomposite could be reused successfully at least for five reaction cycles as shown in Figure 10C.

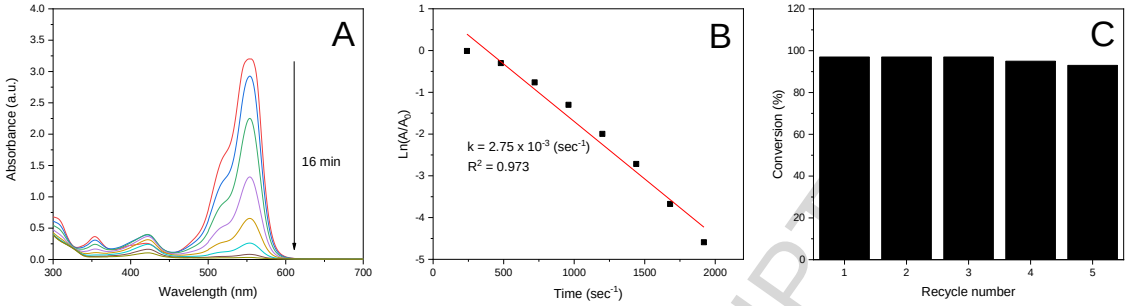

Figure 10. (A) UV-Vis spectra of rhodamine B degradation, (B) First order kinetic plotted and (C) Conversion efficiency of rhodamine B for 5 successive reaction cycles in 16 min.

3.4.Catalytic performance for Sonogashira Coupling

The Pd-catalyzed Sonogashira cross-coupling reactions between aryl halides and acetylenic molecules is one of the most extensively studied reactions in organic synthesis. The use of aqueous media in Pd-catalyzed reactions has received considerable attention because water based synthetic processes are inherently non-toxic, non-flammable and inexpensive [55]. On the other hand, the prepared nanocomposite contains HPCD molecules that can form inclusion complexes by taking up the small molecules into the apolar central cavity and no covalent bonds are formed or broken during complex formation [21]. Therefore, the nanocomposite catalyst is expected to accelerate interaction of insoluble small molecules in the aqueous medium.

To evaluate the catalytic activity of the synthesized PdNCs/HPCD/Alg, we performed Sonogashira cross-coupling reaction using phenylacetylene (**1**) and various aryl halides (**2**) as model substrates. In the typical reaction, 0.11 mmol of phenylacetylene (1.1 equiv.) and 0.1 mmol of aryl halide (1.0 equiv.) was mixed in aqueous solution of the nanocomposite (5 mg) and K_2CO_3 used as base in the air atmosphere. The cross-coupling product accounted for 100% of the aryl halides as the limiting reagent. Purity of the products was determined

by NMR spectra (Supporting information). In purpose of green-catalyst use, we have investigated the coupling reaction between **1** and iodobenzene with and without PPh_3 or/and CuI. The attempts showed that absence of PPh_3 did not affect the reaction yield whereas the reaction without CuI co-catalyst exhibited a very low yield. It reflects that the formation of the copper acetylide is important process for the Sonogashira coupling in presence of the nanocomposite catalyst [56].

Table 2 shows the yield obtained for various aryl iodides in the presence of the composite (5 mg) in the air atmosphere. The results revealed that aryl iodides bearing electron-neutral (Entry 1) and electron-donating (Entries 2 and 3) groups underwent smooth reaction with phenylacetylene in high conversions. For weak electron-withdrawing group like fluoride (Entry 4), the reaction under the nanocomposite catalyst was also maintained in high yield. However, aryl iodides containing the strong electron-withdrawing groups (Entries 5 and 6) displayed the low yields although the extended reaction time at 100°C. A byproduct, 1,4-diphenylbuta-1,3-diyne (Supporting information), which could be formed from coupling two phenyl acetylene molecules in presence of CuI [57], was attributed to dropping the reaction yield of these substituted derivatives.

Table 2. Reaction conditions for Sonogashira reaction in presence of PdNCs/HPCD/Alg in aqueous medium.

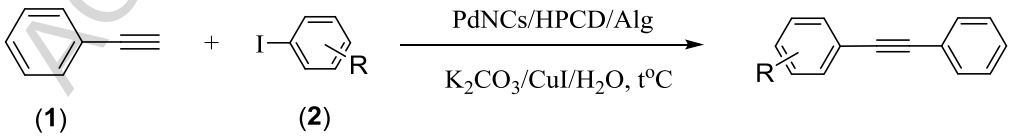

(**1**) (**2**)

Entry	R	Temp. (°C)	Time (h)	Isolated Yield (%)
1	H	80	4	91
2	*p*-CH_3	80	4	92

3	*p*-OCH_3	80	4	90
4	*p*-F	80	4	92
5	*p*-NO_2	100	8	52
6	*m*-CN	100	8	56

In order to check recyclability of the nanocatalyst, we have performed the reusability experiment taking iodobenzene and phenyl acetylene as model substrates in 5 mg of catalyst. Our study revealed that the nanocatalyst could be reused at least for three cycles (Figure 11A). However, a gradual decrease in yield was observed which might be due to the handling loss of the catalyst during collection process. The reused nanocomposite samples were collected for TEM analysis. After reaction, it can see that the particle size distribution of Pd particles were large with a bigger average particle size (14.0 nm), compared to the sample period to reaction (Figure 11B and 11C). Increase of particle size can be attributed to the Oswald ripening process of the catalyst, where atoms detach from thermodynamically unstable smaller clusters and reattach to bigger clusters during the reaction [50, 51]. This nanocomposite showed effectively reusable catalytic activity for Sonogashira coupling in water, compared with catalysts based PdNPs-supported cyclodextrin as previously reported [29, 58, 59].

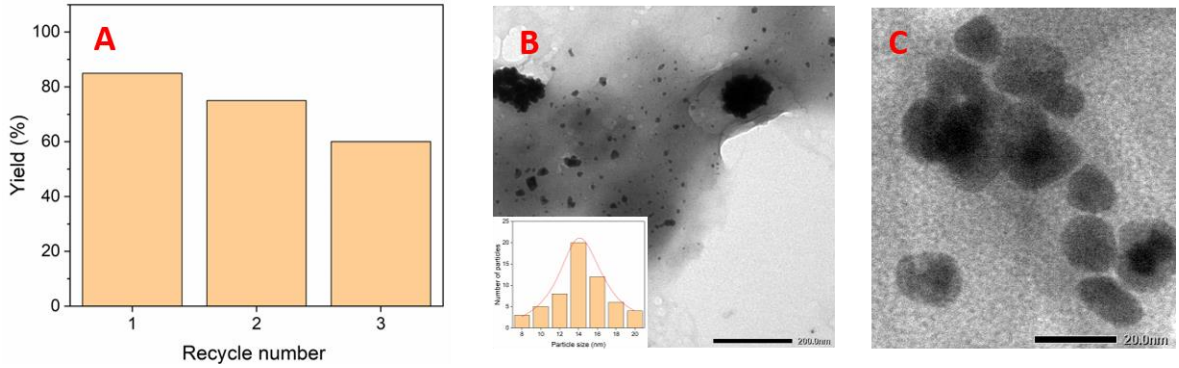

Figure 11. (A) Yields of Sonogashira cross-coupling reaction for three reaction cycles and (B and C) TEM images of the catalyst in different magnifications after three reaction cycles.

4. Conclusions

In this study, we developed an efficient method to trap Pd^{2+} ions by polysaccharides-based nanocomposite via the ionotropic gelation mechanism. PdNCs can be simply synthesized using aqueous extract of *A. lappa* as the reducing agent. The nanocomposite showed excellently recyclable catalyst for the degradation of pollutants and Sonogashira cross-coupling reaction in water medium. For recyclable catalytic degradation of pollutants including 4-nitrophenol, methyl orange and rhodamine B by $NaBH_4$ showed very fast reaction and value of the pseudo-first order rate constants were found from 1.78×10^{-3}, 2.24×10^{-3} and 2.75×10^{-3} sec^{-1}, respectively. Catalytic mechanism of PdNCs for degradation of 4-nitrophenol was found to be a leaching process to form separate particles without recombination into new clusters. Meanwhile, recyclable PdNCs catalyst for Sonogashira cross-coupling reaction acted via the Oswald ripening process. The method used low-cost procedures and friendly-environmental materials that should be considered as a green approach for treatment of pollutants in industrial wastewater.

Disclosure statement.

No potential conflict of interest was reported by the authors.

References

1. P. D. Shankar, S. Shobana, I. Karuppusamy, A. Pugazhendhi, V.S. Ramkumar, S. Arvindnarayan, G. Kumar. A review on the biosynthesis of metallic nanoparticles (gold and silver) using bio-components of microalgae: Formation mechanism and applications. Enzyme Microb. Technol. 95 (2016), 28-44.

2. V. Pareek, A. Bhargava, R. Gupta, N. Jain, J. Panwar. Synthesis and Applications of Noble Metal Nanoparticles: A Review. Advanced Science, Engineering and Medicine 9 (2017), 527-544

3. T. T. Isimjan, Q. He, Y. Liu, J. Zhu, R. J. Puddephatt, D. J. Anderson. Nanocomposite Catalyst with Palladium Nanoparticles Encapsulated in a Polymeric Acid: A Model for Tandem Environmental Catalysis, ACS Sustainable Chem. Eng. 1 (2013), 381–388.

4. A. Bej, K. Ghosh, A. Sarkar, D. W. Knight. Palladium nanoparticles in the catalysis of coupling reactions, RSC Adv. 6 (2016) 11446-11453.

5. G. Blanita, M. D. Lazar. Review of Graphene-Supported Metal Nanoparticles as New and Efficient Heterogeneous Catalysts, Micro and Nanosystems, 5 (2013), 138-146.

6. T. D. Nguyen, V.S. Dang, V.H. Nguyen, T. M. T. Nguyen, C. H. Dang, Synthesis and Photophysical Characterization of Several 2,3-Quinoxaline Derivatives: An Application of Pd(0)/PEG Nanoparticle Catalyst for Sonogashira Coupling, Polycycl. Aromat. Comp. 38 (2018) 42-50.

7. I. I. Moiseev, M. N. Vargaftik. Pd cluster catalysis: a review of reactions under anaerobic conditions**,** New J. Chem. 22 (1998) 1217-1227.

8. X. Li, T. W Goh, C. Xiao, A. L. D. Stanton, Y. Pei, P.K. Jain, W. Huang. Synthesis of Monodisperse Palladium Nanoclusters Using Metal–Organic Frameworks as Sacrificial Templates, ChemNanomat, 2 (2016) 810-815.

9. A. Khalafi-Nezhad, F. Panahi. Immobilized palladium nanoparticles on a silica–starch substrate (PNP–SSS): as an efficient heterogeneous catalyst for Heck and copper-free Sonogashira reactions in water, Green Chem.**,** 13 (2011) 2408-2415.

10. A. Dewan, P. Bharali, U. Bora, A. J. Thakur. Starch assisted palladium(0) nanoparticles as *in situ* generated catalysts for room temperature Suzuki–Miyaura reactions in water**,** RSC Adv. 6 (2016) 11758-11762.

11. M. Tukhani, F. Panahi, A. Khalafi-Nezhad. Supported Palladium on Magnetic Nanoparticles–Starch Substrate (Pd-MNPSS): Highly Efficient Magnetic Reusable Catalyst for C–C Coupling Reactions in Water, ACS Sustainable Chem. Eng., 6 (2018), 1456–1467.

12. M. M. Solomon, H. Gerengi, S. A. Umoren. Carboxymethyl Cellulose/Silver Nanoparticles Composite: Synthesis, Characterization and Application as a Benign Corrosion Inhibitor for St37 Steel in 15% H_2SO_4 Medium. ACS Appl. Mater. Interfaces, 9 (2017), 6376–6389.

13. Z. Lu, J. B. Jasinski, S. Handa, G. B. Hammond. Recyclable cellulose-palladium nanoparticles for clean cross-coupling chemistry**.** Org. Biomol. Chem., 16 (2018) 2748-2752.

14. B.H. Kim , S.Y. Kim, H.G. Woo, J. Jun, H. Sohn. Preparation and Characterization of Silver Nanoparticles in the Presence of Inclusion Complex of b-Cyclodextrin with Phenylsilane. J. Nanosci. Nanotechnol. 8 (2008) 5356–5359.

15. A. Khalafi-Nezhad, F. Panahi. Size-Controlled Synthesis of Palladium Nanoparticles on a Silica–Cyclodextrin Substrate: A Novel Palladium Catalyst System for the Heck Reaction in Water. ACS Sustainable Chem. Eng., 2 (2014) 1177–1186.

16. R. Martin-Trasanco, R. Cao, H.E. Esparza-Ponce, M.E. Montero-Cabrera, R. Arratia-Perez. Reduction of Au(III) by a β-cyclodextrin polymer in acid medium. A stated unattainable reaction, Carbohydr Polym., 175 (2017) 530-537.

17. A.M. Fayaz, K. Balaji, M. Girilal, P.T. Kalaichelvan, R. Venkatesan. Mycobased synthesis of silver nanoparticles and their incorporation into sodium alginate films for vegetable and fruit preservation. J. Agric. Food Chem., 57 (2009) 6246–6252.

18. N. Eghbalifam, M. Frounchi, S. Dadbin. Antibacterial silver nanoparticles in polyvinyl alcohol/sodium alginate blend produced by gamma irradiation. Int. J. Biol. Macromol., 80 (2015) 170–176.

19. M. Faried, K. Shameli, M. Miyake, A. Hajalilou, A. Zamanian, Z. Zakaria, E. Abouzari-lotf, H. Hara, N.B.B.A. Khairudin, M.F.B.M. Nordin. A Green Approach for the Synthesis of Silver Nanoparticles Using Ultrasonic Radiation's Times in Sodium Alginate Media: Characterization and Antibacterial Evaluation. J. Nanomater., 2016 (2016), ID 4941231

20. W.P. Hu, B. Zhang, J. Zhang, W.L. Luo, Y. Guo, S.J. Chen, M.J. Yun, S. Ramakrishna, Y.Z. Long. Ag/alginate nanofiber membrane for flexible electronic skin. Nanotechnology 28 (2017) 445502-445516.

21. T. Huang, F. Meng, L. Qi. Controlled Synthesis of Dendritic Gold Nanostructures Assisted by Supramolecular Complexes of Surfactant with Cyclodextrin. Langmuir 26 (2010) 7582–7589.

22. L. Tarusha, S. Paoletti, A. Travan, E. Marsich. Alginate membranes loaded with hyaluronic acid and silver nanoparticles to foster tissue healing and to control bacterial contamination of non-healing wounds. J. Mater. Sci. Mater. Med. 29 (2018) 22

23. Z. Liu, Q. Xue, Y. Guo. Sensitive electrochemical detection of rutin and isoquercitrin based on SH-β-cyclodextrinfunctionalized graphene-palladium nanoparticles. Biosens. Bioelectron, 89 (2017) 444-452.

24. L. Wang, J. Lei, R. Ma, H. Ju. Host-guest interaction of adamantine with a β-cyclodextrin-functionalized AuPd bimetallic nanoprobe for ultrasensitive electrochemical immunoassay of small molecules. Anal. Chem., 85 (2013), 6505-10.

25. J.D. Senra, L.F.B. Malta, M.E.H.M.D. Costa, R.C. Michel, L.C.S. Aguiar, A.B.C. Simas, O.A.C. Antunes. Hydroxypropyl-α-Cyclodextrin-capped palladium nanoparticles: Active scaffolds for efficient carbon-carbon bond forming cross-coupling in water. Adv. Synth. Catal. 351 (2009) 2411-2422.

26. X. Zhao, X. Liu, M. Lu, M. β-cyclodextrin-capped palladium nanoparticle catalyzed ligand-free Suzuki and Heck couplings. Appl. Organometal. Chem. 28 (2014) 635-640.

27. J. Alvarez, J. Liu, E. Roman, A.E. Kaifer. Water-soluble platinum and palladium nanoparticles modified with thiolated. Chem. Commun. 2000 (2000) 1151–1152.

28. L. Strimbu, J. Liu, A.E. Kaifer. Cyclodextrin-Capped Palladium Nanoparticles as Catalysts for the Suzuki Reaction. Langmuir 19 (2003) 483-485.

29. C. Xue, K. Palaniappan, G. Arumugam, S.A. Hackney, J. Liu, H. Liu. Sonogashira reactions catalyzed by water-soluble, β-cyclodextrin-capped palladium nanoparticles. Catal Letters 116 (2007) 94-100.

30. J. Valdez, I. Gómez. One-Step Green Synthesis of Metallic Nanoparticles Using Sodium Alginate. J. Nanomater, 2016 (2016), ID 9790345.

31. T. Hennebel, P. Verhagen, H. Simoen, B.D. Gusseme, S.E. Vlaeminck, N. Boon, W. Verstraete. Remediation of trichloroethylene by bio-precipitated and encapsulated palladium nanoparticles in a fixed bed reactor. Chemosphere 76 (2009) 1221–1225.

32. B. Hosseinkhani, T. Hennebel, N. Boon. Potential of biogenic hydrogen production for hydrogen driven remediation strategies in marine environments. N. Biotechnol., 31 (2014) 445-50.

33. J. Chang, H. Woo, M.S. Ko, J. Lee, S. Lee, S.T. Yun, S. Lee. Targeted removal of trichlorophenol in water by oleic acid-coated nanoscale palladium/zero-valent iron alginate beads, J. Hazard Mater., 293 (2015) 30-36.

34. T.D. Nguyen, T. H. N. Tran, C.H. Nguyen, C. Im, C.H. Dang. Synthesis and Characterization of β-Cyclodextrin/alginate Nanoparticle as a Novel Drug Delivery System, Chem. Biochem. Eng. Q., 29, 429–435.

35. T.D. Nguyen, C.H. Dang, D.T. Mai. Biosynthesized AgNP capped on novel nanocomposite 2-hydroxypropyl-β-cyclodextrin/alginate as a catalyst for degradation of pollutants. Carbohydr. Polym., 197 (2018) 29-37.

36. T.T.N. Nguyen, T.T. Vo, B.N.H. Nguyen, D.T. Nguyen, V.S. Dang, C.H. Dang, T.D. Nguyen, Silver and gold nanoparticles biosynthesized by aqueous extract of burdock root, *Arctium Lappa* as antimicrobial agent and catalyst for degradation of pollutants, Environ. Sci. Pollut. R (2018). DOI: 10.1007/s11356-018-3322-2

37. Corbett, J.F. Pseudo first-order kinetics. J. Chem. Educ. 49 (1972) 663.

38. C. H. Dang, T.D. Nguyen. Physicochemical characterization of Robusta coffee ground spent oil for biodiesel manufacturing. Waste Biomass Valorization (2018). DOI: 10.1007/s12649-018-0287-9

39. Y.S. Chan, L.N. Cheng, J.H. Wu, E. Chan, Y.W. Kwan, S.M.Y. Lee, G.P.H. Leung, P.H.F. Yu, S.W. Chan. A review of the pharmacological effects of Arctium lappa (burdock). Inflammopharmacol 19 (2011) 245–254.

40. D. Tousch, L.P.R. Bidel, G. Cazals, K. Ferrare, J. Leroy, M. Faucanie, H. Chevassus, M. Tournier, A.D. Lajoix, J. Azay-Milhau. Chemical Analysis and Antihyperglycemic Activity of an Original Extract from Burdock Root (Arctium lappa). J. Agric. Food Chem. 62 (2014) 7738−7745.

41. J. D. Clogston, A.K. Patri. Zeta potential measurement. Methods Mol Biol., 697 (2011), 63–70.

42. T. N. T. Nguyen, T. N. N. Huynh, V.T. Tran, C. H. Dang, T. K. D. Hoang, T. D. Nguyen. Physicochemical characterization, bioactivity evaluation of essential oil from *Citrus microcarpa* Bunge flower and leaf, J. Essent. Oil Res., 30 (4), 2018, 285-292.

43. L. Ai, J. Jiang. Catalytic reduction of 4-nitrophenol by silver nanoparticles stabilized on environmentally benign macroscopic biopolymer hydrogel, Bioresour. Technol., 132 (2013) 374–377.

44. Y. Zhao, H. Zhu, Q. Zhu, Y. Huang, Y. Xia. Three-in-One: Sensing, Self-Assembly and Cascade Catalysis of Cyclodextrin Modified Gold Nanoparticles. J. Am. Chem. Soc., 138 (2016) 16645–16654.

45. S. Lebaschi, M. Hekmati, H. Veisi. Green synthesis of palladium nanoparticles mediated by black tea leaves (Camellia sinensis) extract: Catalytic activity in the reduction of 4-nitrophenol and Suzuki-Miyaura coupling reaction under ligand-free conditions. J. Colloid Interface Sci. 485 (2017) 223–23.

46. D. Berillo, A. Cundy. 3D-macroporous chitosan-based scaffolds with in situ formed Pd and Pt nanoparticles for nitrophenol reduction. Carbohydr Polym., 192 (2018), 166-175.

47. E. Murugan, G. Vimala. Synthesis, characterization, and catalytic activity for hybrids of multi-walled carbon nanotube and amphiphilic poly (propyleneimine) dendrimer immobilized with silver and palladium nanoparticle. J. Colloid Interface Sci., 396 (2013) 101-111

48. F. Christoffel, T. R. Ward. Palladium-Catalyzed Heck Cross-Coupling Reactions in Water: A Comprehensive Review. Catal. Letters, 148 (2018), 489–511.

49. A. Howard, C. E. J. Mitchell, R. G. Egdell. Real time STM observation of Ostwald ripening of Pd nanoparticles on TiO_2 (1 1 0) at elevated temperature. Surf. Sci., 515 (2002), L504-L508.

50. R. Narayanan, M. A. El-Sayed, Effect of Catalysis on the Stability of Metallic Nanoparticles: Suzuki Reaction Catalyzed by PVP-Palladium Nanoparticles. J. Am. Chem. Soc. 125 (2003), 8340-8347.

51. M. B. Thathagar, P. J. Kooyman, R. Boerleider, E. Jansen, C. J. Elsevier, G. Rothenberg. Palladium Nanoclusters in Sonogashira Cross-Coupling: A True Catalytic Species? Adv. Synth. Catal. 347 (2005), 1965 – 1968.

52. C. Kastner, A. F. Thunemann. Catalytic Reduction of 4-Nitrophenol Using Silver Nanoparticles with Adjustable Activity. Langmuir, 32 (2016) 7383–7391.

53. R. Begum, Z. H. Farooqi, E. Ahmed, K. Naseem, S. Ashraf, A. Sharif, R. Rehan. Catalytic reduction of 4- nitrophenol using silver nanoparticles- engineered poly(N-isopropylacrylamide- co- acrylamide) hybrid microgels. Appl Organomet Chem., 31 (2017), e3563.

54. S. Joseph, B. Mathew. Facile synthesis of silver nanoparticles and their application in dye degradation. Materials Science and Engineering: B, 195 (2015), 90–97.

55. M. Lamblin, L. N. Hardy, J. C. Hierso, E. Fouquet, F.X. Felpin. Recyclable Heterogeneous Palladium Catalysts in Pure Water: Sustainable Developments in Suzuki, Heck, Sonogashira and Tsuji–Trost Reactions, Adv. Synth. Catal. 352 (2010) 33-79.

56. R. D. Stephens, and C. E. Castro, The Substitution of Aryl Iodides with Cuprous Acetylides. A Synthesis of Tolanes and Heterocyclics, J. Org. Chem., 28 (1963), 3313–3315.

57. M. B. Smith, J. March. March's advanced organic chemistry reactions, mechanisms, and structure, Wiley & Sons, 904-981 (2007).

58. S. Sadjadi, Palladium nanoparticles immobilized on cyclodextrin- decorated halloysite nanotubes: Efficient heterogeneous catalyst for promoting copper- and ligand- free Sonogashira reaction in water–ethanol mixture, Appl. Organometal. Chem. 32 (2018), e4211.

59. X. Zhao, X. Liu, M. Lu, β- cyclodextrin- capped palladium nanoparticle- catalyzed ligand- free Suzuki and Heck couplings in low- melting β- cyclodextrin/NMU mixtures, 28 (2014), 635-640.

Highlights

- Biogenic PdNCs/HPCD/Alg first synthesized by aqueous extract of *Arctium lappa*
- Characterization of the nanocomposite determined by modern analytic technology
- Recyclable catalytic activity of PdNCs performed for degradation of pollutants
- Recyclable catalytic activity of PdNCs performed for Sonogashira reaction in water